Distribution Agreement

In presenting this thesis or dissertation as a partial fulfillment of the requirements for an advanced degree from Emory University, I hereby grant to Emory University and its agents the non-exclusive license to archive, make accessible, and display my thesis or dissertation in whole or in part in all forms of media, now or hereafter known, including display on the world wide web. I understand that I may select some access restrictions as part of the online submission of this thesis or dissertation. I retain all ownership rights to the copyright of the thesis or dissertation. I also retain the right to use in future works (such as articles or books) all or part of this thesis or dissertation.

Signature:

_____ _____

Carson Telford Date

Geostatistical Modelling and Prediction of Rift Valley Fever Seroprevalence Among Livestock in Uganda

By

Carson Telford

Master of Public Health

Department of Epidemiology

_____

Uriel Kitron, PhD

Committee Chair

_____

Lance Waller, PhD

Committee Member

_____

Trevor Shoemaker, PhD, MPH

Committee Member

Comments

Degree: Master of Public Health

Department: Epidemiology

Committee Chair: Uriel Kitron, PhD

Committee Members: Lance Waller, PhD; Trevor Shoemaker, PhD

Geostatistical Modelling and Prediction of Rift Valley Fever Seroprevalence Among Livestock in Uganda

By

Carson Telford

BS Public Health
Brigham Young University
2019

Thesis Committee Chair: Uriel Kitron, PhD

An abstract of
A thesis submitted to the Faculty of the
Rollins School of Public Health of Emory University
In partial fulfillment of the requirements for the degree of
Master of Public Health
In the Department of Epidemiology
2021

Comments:

Previous Academic Degree: B.S., Brigham Young University, 2019

Thesis Committee Chair: Uriel Kitron

Name of chair, degree: Uriel Kitron, PhD

Master of Public Health or Master of Science in Public Health: Master of Public Health

Department or Program: Epidemiology

Year: 2021

Abstract

Geostatistical Modelling and Prediction of Rift Valley Fever Seroprevalence Among Livestock in Uganda

By: Carson Telford

Background: Rift Valley Fever (RVF) is a mosquito-borne viral hemorrhagic fever endemic to countries throughout the African continent. Uganda is bordered by three endemic countries (Kenya, Tanzania, and South Sudan). Recent outbreak investigations in Uganda indicate the undetected circulation of the virus among both humans and livestock.

Methods: To determine the extent of viral circulation within the country, sampling for antibodies to RVF was carried out among herds of domesticated livestock across 28 districts in Uganda. Environmental variables were evaluated to determine their associations with RVF seroprevalence, and a final geostatistical model was fit to determine covariate and covariance parameters using model-based geostatistics. Model parameters were used to estimate RVF seroprevalence across the country for the year 2017. A map was also produced visualizing the probability that RVF seroprevalence exceeded 15% in each prediction location.

Results: Variables resulting in the best fit to sampling data of RVF seroprevalence included distance to the nearest river, distance to aquatic vegetation, standard deviation of enhanced vegetation index (EVI) over time, percent change in the standard deviation of EVI, and percent change in population density. Predicted RVF seroprevalence was highest in the Northwestern quadrant of the country, along with smaller regions in the South near the border of Rwanda and Tanzania, and in the East near the border of Kenya and North of Lake Victoria. There was high probability that RVF seroprevalence exceeded 15% in areas of high predicted seroprevalence, and low probability that RVF seroprevalence exceeded 15% in most locations in the Northeastern and Southwestern quadrants of the country.

Conclusion: Elevated RVF seroprevalence was strongly associated with proximity to water and high variability in vegetation. Variables representing change over time in population density and variation in vegetation suggest a strong correlation between increased viral circulation and anthropogenic environmental. These results highlight specific locations in which future disease sampling and surveillance efforts should be prioritized to mitigate the risk of future RVF outbreaks.

Geostatistical Modelling and Prediction of Rift Valley Fever Seroprevalence Among Livestock in Uganda

By

Carson Telford

BS Public Health
Brigham Young University
2019

Thesis Committee Chair: Uriel Kitron, PhD

A thesis submitted to the Faculty of the
Rollins School of Public Health of Emory University
in partial fulfillment of the requirements for the degree of
Master of Public Health
in the Department or Epidemiology
2021

Table of Contents

Abstract

Geostatistical Modelling and Prediction of Rift Valley Fever Seroprevalence Among Livestock in Uganda

By: Carson Telford

Background: Rift Valley Fever (RVF) is a mosquito-borne viral hemorrhagic fever endemic to countries throughout the African continent. Uganda is bordered by three endemic countries (Kenya, Tanzania, and South Sudan), and outbreak investigations indicate the undetected circulation of the virus among both humans and livestock.

Methods: To determine the extent of viral circulation within the country, sampling for antibodies to RVF was carried out among herds of domesticated livestock across 28 districts in Uganda. Environmental variables were evaluated to determine their associations with RVF seroprevalence, and a final geostatistical model was fit to determine covariate and covariance parameters using model-based geostatistics. Model parameters were used to estimate RVF seroprevalence across the country for the year 2017. A map was also produced visualizing the probability that RVF seroprevalence exceeded 15% in each prediction location.

Results: Variables resulting in the best fit to sampling data of RVF seroprevalence included distance to the nearest river, distance to aquatic vegetation, standard deviation of enhanced vegetation index (EVI) over time, percent change in the standard deviation of EVI, and percent change in population density. Predicted RVF seroprevalence was highest in the Northwestern quadrant of the country, along with smaller regions in the South near the border of Rwanda and Tanzania, and in the East near the border of Kenya and North of Lake Victoria. There was high probability that RVF seroprevalence exceeded 15% in areas of high predicted seroprevalence, and low probability that RVF seroprevalence exceeded 15% in most locations in the Northeastern and Southwestern quadrants of the country.

Conclusion: Elevated RVF seroprevalence was strongly associated with proximity to water and high variability in vegetation. Variables representing change over time in population density and variation in vegetation suggest a strong correlation between increased viral circulation and anthropogenic environmental change. These results highlight specific locations in which future disease sampling and surveillance efforts should be prioritized to mitigate the risk of future RVF outbreaks.

Introduction

Rift Valley Fever (RVF) is a mosquito-borne zoonotic disease that was discovered in the Great Rift Valley of Africa in the 1930's (1). It is caused by the Rift Valley Fever virus (RVFV), an RNA virus in the family *Bunyaviridae*, genus *Phlebovirus*. Since its discovery, its geographic range has expanded throughout the African continent and its surrounding islands, and the middle eastern countries of Saudia Arabia and Yemen (2–4) and has the potential to continue to spread to new continents (5,6).

RVF has important implications for both animal and human health. To domesticated livestock, RVF has the potential to cause large scale outbreaks with mortality rates of 5-20% in adults and 80-100% in newborns and developing fetuses (1,3,7,8). While livestock vaccines have been developed and can provide immunity to inoculated animals, a recent survey among livestock owners in Kenya and Uganda reported several perceived barriers to vaccination such as monetary cost (direct and indirect), lack of access to information on vaccination, and excessive distance to vaccination sites (9). Infections among humans are usually less severe than in livestock, and thousands of asymptomatic or mild infections in humans likely go undetected (10,11). Common symptoms mirror those of influenza or malaria (12,13). Severe symptoms such as hepatitis, retinitis, encephalitis, or bleeding in the stool and nose occur in about 10% of human infections, and approximately 1% of human infections progress to hemorrhagic disease (1,3). The case fatality rate among humans who develop hemorrhagic disease is 50% (14).

Several vector and zoonotic species play important and unique roles in RVF transmission. Primary vectors of RVF are floodwater *Aedes* mosquitoes, particularly *Ae. mcintoshi* and *Ae. ochraceus*, which can vertically transmit the virus transovarially to their offspring, and horizontally by biting susceptible animals and humans (15). Floodwater mosquito eggs can survive for years in dry soils until heavy rainfall causes flooding, causing dormant mosquito eggs to hatch, some of which may carry the virus and infect nearby susceptible mammalian hosts that act as amplifiers to the virus (16–18). Secondary vectors are those that spread the virus horizontally by transferring RVFV from infected to susceptible hosts when taking blood meals. *Culex pipiens* and *Culex poicilipes* are among secondary vectors with the greatest ability to transmit the virus (19), though other species from the *Culex*, *Anopheles*, *Mansonia*, *Coquillettidia*, and *Eretmapodites* genera are also capable of spreading the virus (5,6,15,19). Enzootic transmission of RVF between biting mosquito vectors and reservoir animal hosts is known to occur at low levels among both domestic and wild ruminants, though infection among wild ruminants is less severe (17,20–22). A confirmed mammal reservoir of the virus has yet to be identified (17,20,21). Human RVF infection can occur from the bite of an infected mosquito, but more commonly occurs via zoonotic transmission through exposure to an infected animal or a product derived from an infected animal (14,22,23). Previously identified risk factors for human RVF infection include handling of livestock or animal products, butchering animal meats, consumption of raw milk, and contact with infected livestock or their aborted fetuses (4,8,14,22–26).

RVF transmission is associated with environmental conditions suitable for mosquito reproduction. Given the key role of vertical transmission in maintaining the RVF virus life cycle, El Niño Southern Oscillation (ENSO) patterns that cause anomalous precipitation and flooding are strongly associated with RVF outbreaks as they initiate the hatching of dormant vertically infected *Aedes* eggs (4,8,16,27–30). Often associated with ENSO patterns, enhanced vegetation index (EVI) satellite remote sensing data can be used to predict RVF outbreaks, as unusually high levels of "greenness" in vegetation are indicative of large amounts of precipitation and suitable environmental conditions for widespread mosquito breeding and subsequent viral transmission (27–29). Other considerations for optimal mosquito habitat and RVF outbreak risk include temperature, elevation, land gradient, soil type, land-use, wild and domesticated animal density, and distance to water sources (4,22,27,29–35).

Uganda is not currently considered a country with endemic RVF, though it is bordered by the endemic countries of Tanzania, Kenya, and South Sudan (3), presenting a potential risk for future increases in RVF infections and establishment of the virus in the country. The area of highest susceptibility to large livestock outbreaks of RVF is termed the "Cattle Corridor," which stretches from the Southwest corner of the country to the Northeast corner and contains approximately 90% of the cattle and other domesticated livestock in Uganda (36,37) (Figure 1). In 2016, the first laboratory confirmed outbreak of RVF in Uganda in 48 years was reported in the Kabale District, where two humans died and four were infected (14,38). In response to these identified cases, serosurveys of humans and animals across the Kabale District were conducted, finding RVF antibodies

in 12% of humans and 13% of animals. Only two humans with active infection were identified via polymerase chain reaction, indicating the undetected circulation of the virus prior to the outbreak. Between 2016-2020, 43 cases of human RVF infections have been confirmed, among whom 22 have died, spanning twenty districts; most in the Cattle Corridor (L. Nyakarahuka, personal communication, February 2, 2021).

Following to the identification of RVF transmission in recent years, we sampled animals from herds of cattle, sheep, and goats (hereby referred to as livestock) for antibodies to RVF in 28 districts throughout Uganda to evaluate the current distribution of RVF. A geostatistical model of livestock seroprevalence and environmental predictors was used to estimate RVF seroprevalence on a grid of the country for the year sampling was conducted. A map was also created to visualize the probability that the seroprevalence of RVF exceeded 15%. Exceedance of 15% seroprevalence was of interest because most studies in endemic countries have shown an average seroprevalence range of 10-20% (17). Regions with high predicted prevalence can be targeted to increase surveillance for future incidence, prioritize livestock RVF vaccine distribution, increase community education, and direct future sampling efforts to validate the results of this analysis and gather necessary additional data to improve accuracy in areas of uncertainty.

Methods

Ethical Statement

The Uganda Virus Research Institute (UVRI) in collaboration with the Viral Special Pathogens Branch at the Centers for Disease Control and Prevention received permission from the Uganda Ministry of Health to gather blood samples from livestock to prevent future morbidity and mortality from RVF. Ethical approval for this study was granted from review by the UVRI Research Ethics Committee (UVRI REC: GC/127/16/03/551). Animal subjects work was conducted according to Uganda national guidelines and performed by officers from the Ministry of Agriculture, Animal Industries and Fisheries.

Livestock Sampling Data

Cross sectional sampling of livestock was conducted between February 2017 to August 2017. Blood samples were collected from 3,181 animals selected from herds at 112 sites in 28 of 134 districts in Uganda. Selection of sampling locations targeted the various geographies within the country and border districts where importation of the virus could occur from neighboring endemic countries. Samples were collected by a team from UVRI. For each herd represented, a random sample of animals was selected from which to collect a blood sample for serological testing.

Environmental Variables

Suitable environments for RVF transmission are made up of complex interactions between climatic, geographic, hydrologic, and geologic variables in combination with anthropogenic considerations such as human and livestock density, urbanization,

agriculture, pastoralism, and land-use change. Spatial data on these variables were obtained on a raster grid of Uganda and values were extracted at sampling locations to determine the association between RVF seroprevalence. Covariate data were downloaded and analyzed at a spatial resolution of $1km^2$, and data unavailable for download in this format was resampled using bilinear interpolation or aggregated to match this resolution. Variables were averaged over the 8 years prior to sampling (2009-2016), with the assumption that this is the average lifespan of Ugandan livestock. Bioclimatic variables were sourced from WorldClim[1] (39) and included elevation, average annual precipitation, average precipitation of the wettest month, average annual temperature, and average temperature of the coldest and warmest months. Additional hydrological variables were sourced from WorldPop[1] (40,41) and the Famine Early Warning Systems Network Land Data Assimilation System[2] (42); they included slope, distance to aquatic vegetation, distance to the nearest major waterway, distance to inland water sources, average monthly surface runoff and surface runoff anomalies, and monthly precipitation anomalies. Remote sensing EVI data were collected from NASA MODIS Terra Vegetation Indices[3] (43), with which we created variables representing annual average monthly EVI, EVI during the rainy seasons, and EVI standard deviation (SD) (summarizing the variability of EVI at this location over time). MODIS also provides land cover data with 16 land type classifications (44). Consistent with Redding et al., we consolidated these classifications into 7 categories: forest (MODIS 1-5), shrubland (MODIS 6-7), savannah (MODIS 8-9), grassland (MODIS 10), wetland (MODIS 11),

[1] Downloaded at a spatial resolution of 30-arc seconds[2]
[2] Downloaded at a spatial resolution of 0.1°[2]
[3] Downloaded at a spatial resolution of $1km^2$

anthropogenic (MODIS 12-14), and bare (MODIS 15-16) (33). Soil data representing percent content of clay, silt, sand, gravel, and soil pH were ascertained from the World Harmonized Soil Database[4] (45). Data representing livestock density (cattle, sheep, and goats) were obtained from the Food and Agriculture Organization[5] (46). Wild animal density data were not available, therefore we calculated and analyzed a variable representing distance to the nearest wildlife reserve or sanctuary using data from the Open Sustainability Institute to measure the possible association between RVF seroprevalence and proximity to areas of higher wild animal density (47). Initial anthropogenic variables analyzed included human population density data which were adjusted to match the United Nations population estimates for Uganda sourced from WorldPop (48) and presence of irrigation from HarvestChoice[6] (49). Previous research suggests that environmental changes such as deforestation and land-use change can result in elevated risk for transmission of vector-borne diseases (50–53). To account for these dynamics, we created variables representing the percent change in average annual EVI, the percent change in annual EVI SD, and the percent change in population density over an 8-year period. Percent change in EVI variables was calculated as the change between the average monthly EVI during the four years prior to sampling (2013-2016) and the four years earlier (2009-2012). Percent change in estimated population density was calculated as the change from the year 2012 to 2016. A small proportion of the cells for which percent change was calculated had outlier values due to low initial values, and a

[4] Downloaded at a spatial resolution of 30-arc seconds[2]
[5] Downloaded at spatial resolution of 5-arc minutes[2]
[6] Downloaded at spatial resolution of 5-arc minutes[2]

maximum percent change of 50% was allowed in any given cell to prevent excessive influence of these areas.

Statistical Analysis

Preliminary model selection utilized a non-spatial binomial generalized linear model to identify individual variables with the strongest associations with RVF seroprevalence through bivariate and multivariate analyses. A cutoff of 0.6 was used when evaluating correlation between variables to retain in the model. If a given model had a variance inflation factor of 3 or higher, it was determined that collinearity between covariates was present and the variable of least significance was removed from the model until no evidence of collinearity remained. Covariates associated with RVF (α=0.05) in the non-spatial model were then incorporated into a Generalized Linear Geostatistical Model (GLGM) using Model-based Geostatistics (54). Covariates were tested to identify the best fitting model after accounting for the spatial data structure. Multiple models were compared and the final model was selected based on the log-likelihood value that indicated the best fit to the data. The final model included five covariates: distance to a major waterway (DIST WATERWAY), distance to aquatic vegetation (DIST AQUATIC), EVI SD, percent change in EVI SD (EVI SD % CHG), and percent change in population density (POP DENS % CHG). The GLGM of the probability that a given sampled animal had positive antibodies for RVF was then implemented in the following framework:

$$\text{Log}\{p(x)/[1-p(x)]\} = \beta_0 + \beta_1(\text{DIST WATERWAY}) + \beta_2(\text{DIST AQUATIC}) + \beta_3(\text{EVI SD}) + \beta_4(\text{EVI SD \% CHG}) + \beta_5(\text{POP DENS \% CHG}) + S(x_i) + U_i$$

Where $p(x)$ denotes the prevalence of RVF in location x, β represents the effects of the specified covariates at each prediction location, $S(x)$ represents a spatial random effect which follows a Gaussian process with mean zero and variance σ^2 and a Matern correlation function. The shape parameter of the Matern correlation function was specified as k=1, based on the profile likelihood for the shape parameter in a logit-transformed linear Gaussian model. Covariance parameters were identified by fitting a semi-variogram of model residuals, which represents the decay in correlation between observations as distance between them increases. The "nugget effect" U_i represents the unstructured random variation in the outcome and is included to capture the effects of unmeasured explanatory variables that have little to no spatial structure.

A Bayesian Markov Chain Monte Carlo (MCMC) approach was used to fit our spatial binomial generalized linear mixed model using 100,000 simulations within the *PrevMap* package (55) in R 1.3.1075 version (56). Prediction of RVF seroprevalence was carried out on a $1km^2$ resolution grid (168,857 total cells) of Uganda. Bayesian diffuse priors were used for model parameters because of the variability across the literature regarding associations between RVF, environmental predictors, and covariance parameters.

Prevalence prediction at unsampled locations was based on covariate values in each cell and the correlation structure from the fitted model. Model-based geostatistics uses the

spatial auto-correlation of sampled locations from the empirical semi-variogram to weight the influence that nearby sampled locations have on the predicted values in prediction locations (57). In implementation, if a sampled location has an observed prevalence of RVF that is higher than expected given the model, a spatial smoothing term, S(x), serves to increase the predicted values in nearby surrounding locations, and vice-versa where the observed RVF seroprevalence is lower than would be expected given the model and neighboring values. If a location lies beyond the distance at which observations are correlated (per the semi-variogram), then the prevalence is predicted as the expected value based on the covariates without weights added or subtracted according to surrounding sampling points.

Maps visualizing the predicted RVF seroprevalence and the probability that RVF seroprevalence in a given location exceeded 15% for the year of data collection (2017) were generated using QGIS 3.10 (58). The probability of exceeding 15% was defined as the proportion of times the predicted seroprevalence at a given location exceeded 15% across the MCMC simulations and corresponds to the posterior probability of the local prevalence exceeding 15%. A plot was produced using R 1.3.1075 to visualize the difference between the observed seroprevalence compared to the predicted prevalence in sampled locations by the GLGM (56).

Model Validation

We used Monte Carlo iterations to simulate 1,000 semi-variograms given the fitted model to determine the validity and fit of the spatial correlation structure to the data. A 95% interval defining the variability of the model simulations was used to evaluate whether the model accurately fit the data. The null hypothesis was that the specified model was a good fit to the data. After the simulation, the fitted semi-variogram based on the observed data fell within the 95% interval of variograms estimated from the simulated data, and it was determined that the specified correlation structure adequately fit the data in order to proceed with prediction (57). Convergence of the model was evaluated using trace plots of the MCMC values of each model parameter and correlation plots to ensure retained links in the Markov Chain were not correlated after thinning. Finally, we duplicated the analysis using Monte Carlo Maximum Likelihood to compare to the Bayesian MCMC analysis and confirm consistency between statistical model fitting methods.

Results

Maps of the spatial distributions of each covariate show that major waterways run throughout the country, and that aquatic vegetation is most sparse in Northeast Uganda. EVI SD is generally higher in the Northern half of the country, indicating more stable vegetation coverage in the Southern half, while percent change in EVI SD occurred on a more localized scale in various regions throughout the country. Population density increased most in Northwestern Uganda (Figure 2). The map of predicted RVF seroprevalence among livestock shows notable heterogeneity across the country, and the highest predicted seroprevalence in the Northwestern quadrant of the country from Lake

Albert to the border of South Sudan (Figure 3). Other areas with high predicted prevalence were also located along the outskirts of the lakes in the center of the country (Lake Kyoga and Lake Kwania), on the Southern border near Rwanda and Tanzania, along the North borders of Lake Victoria, and along the border of Kenya. Conversely, the areas with the lowest predicted seroprevalence were in the Northeastern and Southwestern corners of the country, where the predicted seroprevalence generally ranged from 0 to 10%.

The map visualizing the estimated probability that RVF seroprevalence exceeds 15% is presented in Figure 4. Red and orange cells represent areas where there is high probability that the true RVF seroprevalence exceeds 15%, while areas in dark and light green represent areas where this probability is low. Gray cells represent areas of uncertainty, where there is inadequate data to confidently determine whether the true RVF seroprevalence is higher or lower than 15%. Areas of uncertainty most frequently occurred at the intersection between high and low prevalence areas. There was very low probability that RVF seroprevalence exceeded 15% in most of the Northeastern and Southwestern quadrants of Uganda apart from scattered areas of high probability around the southern border and center of the country.

Parameter estimates for the GLGM model in Table 1 show that there were statistically significant associations between RVF logit-prevalence and EVI SD (p=0.04; CI: 1.72, 49.66), EVI SD percent change (p=0.004; CI: 0.0, 0.08), and population density percent change (p=0.006; CI: 0.0, 0.04). Distance to a major waterway and aquatic vegetation

both had inverse relationships with RVF logit-prevalence, however these relationships were not significant using a 95% credible interval.

Some of the herds with the highest unadjusted observed prevalence were those with relatively low sample sizes (Figure 5). Comparing observed prevalence from herds sampled with small sample sizes to the model-predicted prevalence in the same locations, we see that predicted seroprevalence was lower in many instances, being smoothed by the model after accounting for environmental conditions, the spatial structure of surrounding sampling sites, and the standard deviation associated with fewer observations. This is typical behavior for spatial models of disease rates. Areas with small sample sizes yield unstable local rate estimates and the models borrow more information from neighboring sites to stabilize estimates. Most herds with an observed RVF seroprevalence of zero were also those with few animals sampled, and the model predicted seroprevalence was higher than observed in those locations as the model borrows information from neighboring (and often non-zero) values.

Discussion

This analysis provides estimates of RVF seroprevalence in Uganda in 2017 and suggests heterogeneous circulation of RVF throughout the country. Studies of RVF in endemic countries have found a seroprevalence of 10-20% (17). Our results suggest a high probability of RVF circulation (≥15%) in several regions of Uganda, and lower probability in others. The highest predicted seroprevalence was in the Northwestern

quadrant of the country, the focal point being Northeast of Lake Albert. Other areas of high predicted prevalence were around the outskirts of the lakes in the center of the country, on the Southern border near Rwanda and Tanzania, directly North of Lake Victoria, and near the border of Kenya. Comparison between the map of the Cattle Corridor in Figure 1 and the map of predicted RVF prevalence in Figure 3 reveals several areas of overlap between those with high predicted RVF seroprevalence and high livestock density, indicating elevated risk for livestock exposure to RVF and the potential for outbreaks in these locations. Several areas where sampling was not done were identified as locations with high probability of elevated RVF seroprevalence, given the environmental predictors represented in this model and the geographic proximity of sampling locations with elevated seroprevalence. This information can be used to direct future livestock sampling efforts to validate the predictions from this model, and if accurate, can help prioritize future mitigation efforts such as livestock vaccine administration campaigns and public outreach and education on risk factors for RVF transmission. Directing such efforts to specific geographic locations combined with an understanding of the distribution of livestock and temporal trends of RVF outbreaks, such as during ENSO years, can potentially lead to a reduction in the burden of RVF (27–29,59).

The Northwestern region of Uganda, where observed and predicted prevalence was highest, is the site of two national parks (Murchison Falls National Park and Paraa National Park) and two wildlife and game reserves (Aswa-Lolim Game Reserve and Ajai Wildlife Reserve). While this region does not fall within the Cattle Corridor, high RVF

seroprevalence in herds in this region may be attributable to virus circulation between mosquitoes and the high density of wild animals, which typically remain asymptomatic upon infection (60). Interestingly, a large increase in population density also occurred in this region during the years prior to sampling (Figure 2). Given the results of this model, one possible explanation for the elevated RVF seroprevalence in livestock is that increased human presence may have resulted in the opportunity for transfer of the virus from wild animals to newly introduced and immunologically naïve livestock by mosquito vectors. Alternatively, increased livestock trade could potentially have resulted in the importation of animals previously exposed to RVF in other geographical regions. Further research should be conducted to evaluate trade networks and importation of livestock in Northwestern Uganda to determine the location of exposure to RVFV. Analysis of proximity to and interaction between wild animals in nearby game reserves and national parks and livestock in Northwestern Uganda may also provide evidence to support the hypothesis of increased viral circulation in this region. Such information could be used to determine the importance of limiting interaction between livestock and wild animals and prioritizing specific interventions. The observed increase in population density in this region that is comprised of several protected natural areas and game reserves also merits further research and intervention to mitigate the risk of disease spillover events that typically occur as a result of environmental change from deforestation and agricultural expansion (61).

Past research has identified strong correlations between RVF outbreaks, large amounts of precipitation, and high EVI. We found that *variability* in EVI over time, represented by

EVI SD, rather than average EVI or EVI during the rainy seasons, was a stronger indicator of elevated RVF seroprevalence. Studies that have used vegetation indices to successfully predict RVF outbreaks are based on anomalous levels of EVI and rainfall (27–29). Because seroprevalence sampling data cannot determine the time of exposure to RVF, it was not possible to associate specific vegetation or weather anomalies with RVF circulation in this study. However, areas with higher variability in EVI may be those in which anomalous precipitation and vegetation indices more commonly occur. Areas with more variability in EVI may also be at greater risk of RVF transmission because fluctuation in precipitation and vegetation indices throughout the year may represent dryer soil conditions that are more conducive to flooding during the rainy seasons. Percent change in EVI SD also had a strong positive association with RVF seroprevalence, indicating that variability in EVI increased over time in areas with higher seroprevalence. EVI is a measure of the level of greenness of vegetation imaged by satellites and does not identify specific types of vegetation or specifically differentiate between forested or agricultural lands. Increased variability in annual EVI may be an indicator of change from natural vegetation to agricultural land, as "greenness" in crops typically varies more throughout the year than natural vegetation (62–64).

Increases in human presence over time is represented through the percent change in population density, which also had a significant positive association with RVF seroprevalence. Aside from increases in susceptible humans and livestock, population density change can lead to various environmental changes that lead to better habitat suitability for mosquitoes and elevated risk of RVF outbreaks. Land change resulting

from population growth and the introduction of irrigated agriculture can be beneficial for RVF circulation because the flooding of fields can cause dormant infected *Aedes* eggs to hatch, and creates large areas of stagnant water that secondary vectors can use to reproduce (65). Land conversion and deforestation resulting from population growth can also cause disruption of soil absorption and drainage networks, potentially resulting in flooding (66). Though percent change in EVI SD and percent change in population density could potentially represent similar anthropogenic changes to the environment that lead to increased RVF circulation, these variables had a weak correlation, suggesting their encompassment of unique contributions to the dynamics of RVF transmission. Future research should seek to identify the underlying causes of increased EVI variability in areas of higher RVF seroprevalence in Uganda and its relationship with increases in human population density and mosquito reproduction.

Areas of high predicted RVF seroprevalence were identified near the borders between Uganda and all of its bordering countries. These findings suggest the possibility of geographical dispersion of RVF from currently endemic countries to Uganda. This possibility is supported by an RVF serosampling study done in Rwanda, which found RVF seroprevalence of 8-10% in districts bordering Uganda (67), though there is a lack of such evidence for other bordering countries. Phylogenetic analyses should be used to analyze viral strains from Uganda and those in surrounding countries to determine the existence of directionality in geographic dispersion of the virus.

This analysis is subject to several limitations. Livestock density was not directly accounted for, as this variable was found to have little to no association with RVF seroprevalence in the model selection process. Most areas with the highest predicted prevalence in Northwestern Uganda fall outside of the Cattle Corridor. This can potentially be explained by the fact that RVF circulates among both domesticated and wild animals (17,21,60). However, wild animal density was also not directly accounted for in this model as data were not available. Livestock density may indirectly be accounted for within the variables representing increases in population density and EVI SD, as urbanization, land-use change, deforestation, and agriculture may be associated with the introduction of livestock and pastoralism in new areas. Seroprevalence surveys are unable to account for the strong temporal trends associated with RVF outbreaks. We evaluated variables such as average EVI during the rainy seasons and average precipitation anomalies to account for the temporal trends in transmission, but the associations between these variables and RVF seroprevalence were less significant than those used in the final model. To correlate specific weather events with RVF seroprevalence, secondary testing should be conducted to measure changes in RVF seroprevalence and weather events between sampling periods. We found a strong association between RVF seroprevalence and the percent change in population density, however, these population density data are modeled estimates and not census data. To improve accuracy, these data are adjusted to match the United Nations population estimates, which are available in larger subnational units. Finally, the statistical method we used to estimate seroprevalence in each prediction location was multivariate kriging, which requires the assumption of stationarity in the disease transmission process.

Conclusion

This analysis estimated RVF seroprevalence across Uganda in the year 2017 by fitting a geostatistical model to livestock sampling data and environmental predictors. The highest predicted seroprevalence was in the Northwestern quadrant of the country, in the South near the borders of Rwanda and Tanzania, and North of Lake Victoria near the border of Kenya. The lowest predicted seroprevalence was in the Northeastern and Southwestern corners of the country, which encompass a large proportion of Uganda's Cattle Corridor. The variables found to be the best predictors of RVF seroprevalence included proximity to major waterways and aquatic vegetation, high variability in EVI, and change in EVI variability and population density during the 8 years prior to sampling. Variables representing anthropogenic change were found to be the most strongly associated with RVF seroprevalence (Table 1). These results can be used to guide the prioritization of future RVF sampling efforts to confirm our model predictions, and if accurate, the prioritization of surveillance and risk mitigation efforts such as RVF vaccine distribution and community education regarding RVF transmission prevention.

References

1. Daubney R, Hudson JR. Enzootic Hepatitis or Rift Valley Fever. An Un-described Virus Disease of Sheep, Cattle and Man from East Africa. J Pathol Bacteriol. 1931;34:545–79.

2. Gerdes GH. Rift Valley fever. Rev Sci Tech Int Off Epizoot. 2004;23(2):613–23.

3. Rift Valley Fever | CDC [Internet]. 2020 [cited 2021 Apr 10]. Available from: https://www.cdc.gov/vhf/rvf/index.html

4. Himeidan YE, Kweka EJ, Mahgoub MM, El Rayah EA, Ouma JO. Recent outbreaks of rift valley fever in east africa and the middle east. Front Public Health. 2014;2:169.

5. Turell MJ, Dohm DJ, Mores CN, Terracina L, Wallette DL, Hribar LJ, et al. Potential for North American Mosquitoes to Transmit Rift Valley Fever Virus1. J Am Mosq Control Assoc. 2008;24(4):502–7.

6. Turell MJ, Britch SC, Aldridge RL, Kline DL, Boohene C, Linthicum KJ. Potential for mosquitoes (Diptera: Culicidae) from Florida to transmit Rift Valley fever virus. J Med Entomol. 2013;50(5):1111–7.

7. Coetzer JA. The pathology of Rift Valley fever. II. Lesions occurring in field cases in adult cattle, calves and aborted foetuses. 1982;

8. Hartman A. Rift valley fever. Clin Lab Med. 2017;37(2):285–301.

9. Mutua E, de Haan N, Tumusiime D, Jost C, Bett B. A qualitative study on gendered barriers to livestock vaccine uptake in Kenya and Uganda and their implications on Rift Valley Fever control. Vaccines. 2019;7(3):86.

10. Mohamed M, Mosha F, Mghamba J, Zaki SR, Shieh W-J, Paweska J, et al. Epidemiologic and clinical aspects of a Rift Valley fever outbreak in humans in Tanzania, 2007. Am J Trop Med Hyg. 2010;83(2_Suppl):22–7.

11. Nguku PM, Sharif SK, Mutonga D, Amwayi S, Omolo J, Mohammed O, et al. An investigation of a major outbreak of Rift Valley fever in Kenya: 2006–2007. Am J Trop Med Hyg. 2010;83(2_Suppl):05–13.

12. Laughlin LW, Meegan JM, Strausbaugh LJ, Morens DM, Watten RH. Epidemic Rift Valley fever in Egypt: observations of the spectrum of human illness. Trans R Soc Trop Med Hyg. 1979;73(6):630–3.

13. McIntosh BM. Rift Valley fever: 1. Vector studies in the field. J S Afr Vet Assoc. 1972;43(4):391–5.

14. de St. Maurice A, Nyakarahuka L, Purpura L, Ervin E, Tumusiime A, Balinandi S, et al. Rift Valley fever response—Kabale District, Uganda, March 2016. Morb Mortal Wkly Rep. 2016;65(43):1200–1.

15. Linthicum KJ, Davies FG, Kairo A, Bailey CL. Rift Valley fever virus (family Bunyaviridae, genus Phlebovirus). Isolations from Diptera collected during an inter-epizootic period in Kenya. Epidemiol Infect. 1985;95(1):197–209.

16. Linthicum KJ, Britch SC, Anyamba A. Rift Valley fever: an emerging mosquito-borne disease. Annu Rev Entomol. 2016;61:395–415.

17. Clark MH, Warimwe GM, Di Nardo A, Lyons NA, Gubbins S. Systematic literature review of Rift Valley fever virus seroprevalence in livestock, wildlife and humans in Africa from 1968 to 2016. PLoS Negl Trop Dis. 2018;12(7):e0006627.

18. Sang R, Arum S, Chepkorir E, Mosomtai G, Tigoi C, Sigei F, et al. Distribution and abundance of key vectors of Rift Valley fever and other arboviruses in two ecologically distinct counties in Kenya. PLoS Negl Trop Dis. 2017;11(2):e0005341.

19. Turell MJ, Linthicum KJ, Patrican LA, Davies FG, Kairo A, Bailey CL. Vector competence of selected African mosquito (Diptera: Culicidae) species for Rift Valley fever virus. J Med Entomol. 2008;45(1):102–8.

20. Olive M-M, Goodman SM, Reynes J-M. The role of wild mammals in the maintenance of Rift Valley fever virus. J Wildl Dis. 2012;48(2):241–66.

21. Dondona AC, Aschenborn O, Pinoni C, Di Gialleonardo L, Maseke A, Bortone G, et al. Rift valley fever virus among wild ruminants, Etosha National Park, Namibia, 2011. Emerg Infect Dis. 2016;22(1):128.

22. Munyua PM, Murithi RM, Ithondeka P, Hightower A, Thumbi SM, Anyangu SA, et al. Predictive factors and risk mapping for Rift Valley fever epidemics in Kenya. PLoS One. 2016;11(1):e0144570.

23. Nyakarahuka L, Maurice A de S, Purpura L, Ervin E, Balinandi S, Tumusiime A, et al. Prevalence and risk factors of Rift Valley fever in humans and animals from Kabale district in Southwestern Uganda, 2016. PLoS Negl Trop Dis. 2018;12(5):e0006412.

24. Abu-Elyazeed R, El-Sharkawy S, Olson J, Botros B, Soliman A, Salib A, et al. Prevalence of anti-Rift-Valley-fever IgM antibody in abattoir workers in the Nile delta during the 1993 outbreak in Egypt. Bull World Health Organ. 1996;74(2):155.

25. LaBeaud AD, Pfeil S, Muiruri S, Dahir S, Sutherland LJ, Traylor Z, et al. Factors associated with severe human rift valley fever in sangailu, garissa county, kenya. PLoS Negl Trop Dis. 2015;9(3):e0003548.

26. Madani TA, Al-Mazrou YY, Al-Jeffri MH, Mishkhas AA, Al-Rabeah AM, Turkistani AM, et al. Rift Valley fever epidemic in Saudi Arabia: epidemiological, clinical, and laboratory characteristics. Clin Infect Dis. 2003;37(8):1084–92.

27. Linthicum KJ, Anyamba A, Tucker CJ, Kelley PW, Myers MF, Peters CJ. Climate and satellite indicators to forecast Rift Valley fever epidemics in Kenya. Science. 1999;285(5426):397–400.

28. Anyamba A, Chretien J-P, Small J, Tucker CJ, Formenty PB, Richardson JH, et al. Prediction of a Rift Valley fever outbreak. Proc Natl Acad Sci. 2009;106(3):955–9.

29. Anyamba A, Linthicum KJ, Small J, Britch SC, Pak E, de La Rocque S, et al. Prediction, assessment of the Rift Valley fever activity in East and Southern Africa 2006–2008 and possible vector control strategies. Am J Trop Med Hyg. 2010;83(2_Suppl):43–51.

30. Martin V, Chevalier V, Ceccato P, Anyamba A, De Simone L, Lubroth J, et al. The impact of climate change on the epidemiology and control of Rift Valley fever. 2008;

31. Chevalier V, Rakotondrafara T, Jourdan M, Heraud JM, Andriamanivo HR, Durand B, et al. An unexpected recurrent transmission of Rift Valley fever virus in cattle in a temperate and mountainous area of Madagascar. PLoS Negl Trop Dis. 2011;5(12):e1423.

32. Lernout T, Cardinale E, Jego M, Després P, Collet L, Zumbo B, et al. Rift valley fever in humans and animals in Mayotte, an endemic situation? PLoS One. 2013;8(9):e74192.

33. Redding DW, Tiedt S, Lo Iacono G, Bett B, Jones KE. Spatial, seasonal and climatic predictive models of Rift Valley fever disease across Africa. Philos Trans R Soc B Biol Sci. 2017;372(1725):20160165.

34. Tran A, Trevennec C, Lutwama J, Sserugga J, Gely M, Pittiglio C, et al. Development and assessment of a geographic knowledge-based model for mapping suitable areas for Rift Valley fever transmission in Eastern Africa. PLoS Negl Trop Dis. 2016;10(9):e0004999.

35. Métras R, Jewell C, Porphyre T, Thompson PN, Pfeiffer DU, Collins LM, et al. Risk factors associated with Rift Valley fever epidemics in South Africa in 2008–11. Sci Rep. 2015;5(1):1–7.

36. Barihaihi M. Africa Climate Change Resilience Alliance (ACCRA) Uganda. 2010;

37. Stark J, Mataya C. Climate change and conflict in Uganda: the cattle corridor and Karamoja. No Febr. 2011;

38. Shoemaker TR, Nyakarahuka L, Balinandi S, Ojwang J, Tumusiime A, Mulei S, et al. First Laboratory-Confirmed Outbreak of Human and Animal Rift Valley Fever Virus in Uganda in 48 Years. Am J Trop Med Hyg. 2019;100(3):659–71.

39. Fick SE, Hijmans RJ. WorldClim 2: new 1-km spatial resolution climate surfaces for global land areas. Int J Climatol. 2017;37(12):4302–15.

40. Lloyd CT, Sorichetta A, Tatem AJ. High resolution global gridded data for use in population studies. Sci Data. 2017;4(1):1–17.

41. Lloyd CT, Chamberlain H, Kerr D, Yetman G, Pistolesi L, Stevens FR, et al. Global spatio-temporally harmonised datasets for producing high-resolution gridded population distribution datasets. Big Earth Data. 2019 Apr 3;3(2):108–39.

42. McNally A, Arsenault K, Kumar S, Shukla S, Peterson P, Wang S, et al. A land data assimilation system for sub-Saharan Africa food and water security applications. Sci Data. 2017;4(1):1–19.

43. Didan, Kamel. MOD13Q1 MODIS/Terra Vegetation Indices 16-Day L3 Global 250m SIN Grid V006 [Internet]. NASA EOSDIS Land Processes DAAC; 2015 [cited 2021 Apr 10]. Available from: https://lpdaac.usgs.gov/products/mod13q1v006/

44. Friedl, Mark, Sulla-Menashe, Damien. MCD12Q1 MODIS/Terra+Aqua Land Cover Type Yearly L3 Global 500m SIN Grid V006 [Internet]. NASA EOSDIS Land Processes DAAC; 2019 [cited 2021 Apr 10]. Available from: https://lpdaac.usgs.gov/products/mcd12q1v006/

45. Nachtergaele FO, van Velthuizen H, Verelst L, Batjes NH, Dijkshoorn JA, van Engelen VWP, et al. Harmonized world soil database (version 1.0). 2008;

46. Gilbert M, Nicolas G, Cinardi G, Van Boeckel TP, Vanwambeke SO, Wint GW, et al. Global distribution data for cattle, buffaloes, horses, sheep, goats, pigs, chickens and ducks in 2010. Sci Data. 2018;5(1):1–11.

47. Open Sustainability Institute. Uganda Protected Areas [Internet]. Harvard Dataverse; 2017 [cited 2021 Apr 10]. Available from: https://dataverse.harvard.edu/citation?persistentId=doi:10.7910/DVN/BEVMRY

48. WorldPop,, Bondarenko, Maksym. Individual Countries 1km Population Density (2000-2020) [Internet]. University of Southampton; 2020 [cited 2021 Apr 10]. Available from: https://www.worldpop.org/doi/10.5258/SOTON/WP00674

49. International Food Policy Research Institute. Global Spatially-Disaggregated Crop Production Statistics Data for 2010 Version 2.0 [Internet]. Harvard Dataverse; 2019 [cited 2021 Apr 10]. Available from: https://dataverse.harvard.edu/citation?persistentId=doi:10.7910/DVN/PRFF8V

50. Brock PM, Fornace KM, Grigg MJ, Anstey NM, William T, Cox J, et al. Predictive analysis across spatial scales links zoonotic malaria to deforestation. Proc R Soc B. 2019;286(1894):20182351.

51. Taylor D, Hagenlocher M, Jones AE, Kienberger S, Leedale J, Morse AP. Environmental change and Rift Valley fever in eastern Africa: projecting beyond HEALTHY FUTURES. Geospatial Health. 2016;

52. Nakouné E, Kamgang B, Berthet N, Manirakiza A, Kazanji M. Rift Valley fever virus circulating among ruminants, mosquitoes and humans in the Central African Republic. PLoS Negl Trop Dis. 2016;10(10):e0005082.

53. Norris DE. Mosquito-borne diseases as a consequence of land use change. EcoHealth. 2004;1(1):19–24.

54. Diggle PJ, Tawn JA, Moyeed RA. Model-based geostatistics. J R Stat Soc Ser C Appl Stat. 1998;47(3):299–350.

55. Giorgi E, Diggle PJ. PrevMap: an R package for prevalence mapping. J Stat Softw. 2017;78(8):1–29.

56. Team RC. R: A language and environment for statistical computing. 2013;

57. Diggle PJ, Giorgi E. Model-based geostatistics for global public health: methods and applications. CRC Press; 2019.

58. QGIS Development Team. QGIS Geographic Information System. 2021.

59. Breiman RF. Decision-support tool for prevention and control of Rift Valley fever epizootics in the Greater Horn of Africa. Am J Trop Med Hyg. 2010;83(2, Supplement):75–85.

60. Evans A, Gakuya F, Paweska JT, Rostal M, Akoolo L, Van Vuren PJ, et al. Prevalence of antibodies against Rift Valley fever virus in Kenyan wildlife. Epidemiol Infect. 2008;136(9):1261–9.

61. Gillespie TR, Jones KE, Dobson AP, Clennon JA, Pascual M. COVID-Clarity demands unification of health and environmental policy. Glob Change Biol. 2021;27(7):1319–21.

62. Epule TE, Ford JD, Lwasa S, Nabaasa B, Buyinza A. The determinants of crop yields in Uganda: what is the role of climatic and non-climatic factors? Agric Food Secur. 2018;7(1):1–17.

63. Gurgel HC, Ferreira NJ. Annual and interannual variability of NDVI in Brazil and its connections with climate. Int J Remote Sens. 2003;24(18):3595–609.

64. Lobell DB, Azzari G, Burke M, Gourlay S, Jin Z, Kilic T, et al. Eyes in the sky, boots on the ground: assessing satellite-and ground-based approaches to crop yield measurement and analysis in Uganda. World Bank Policy Res Work Pap. 2018;(8374).

65. Muturi EJ, Shililu JI, Gu W, Jacob BG, Githure JI, Novak RJ. Larval habitat dynamics and diversity of Culex mosquitoes in rice agro-ecosystem in Mwea, Kenya. Am J Trop Med Hyg. 2007;76(1):95–102.

66. Surface Runoff and the Water Cycle [Internet]. [cited 2021 Apr 10]. Available from: https://www.usgs.gov/special-topic/water-science-school/science/surface-runoff-and-water-cycle?qt-science_center_objects=0#qt-science_center_objects

67. Gafarasi I, Rukelibuga J, Mushonga B, Umuhoza T, Biryomumaisho S, Berkvens D. Seroprevalence of Rift Valley fever in cattle along the Akagera–Nyabarongo rivers, Rwanda. J S Afr Vet Assoc. 2017;88(1):1–5.

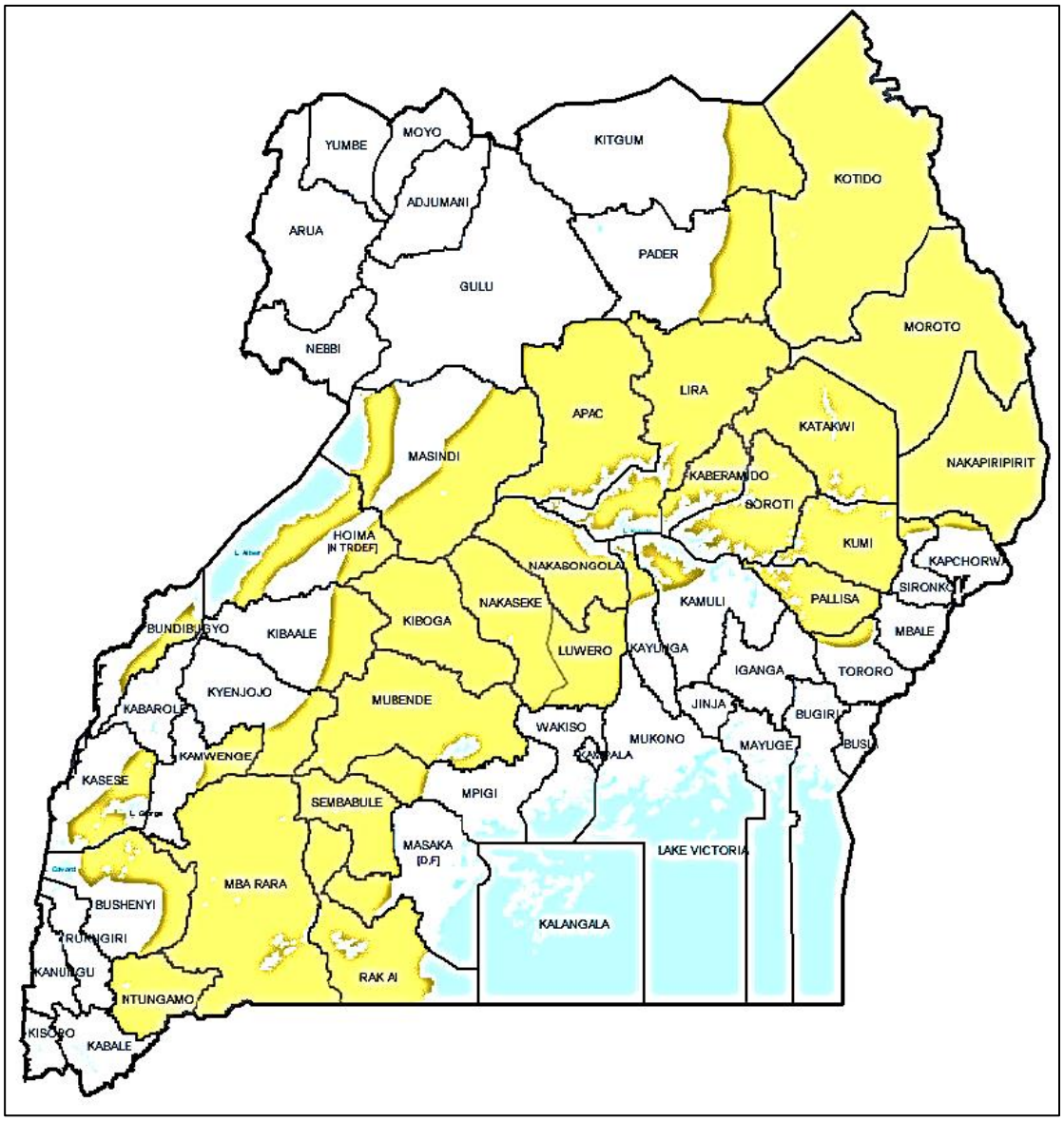

Figure 1. Uganda's Cattle Corridor. Uganda's 134 administrative districts with an overlay of the Cattle Corridor in yellow. The Cattle Corridor contains approximately 90% of the cattle in the country.
Adapted from Barihaihi 2010.

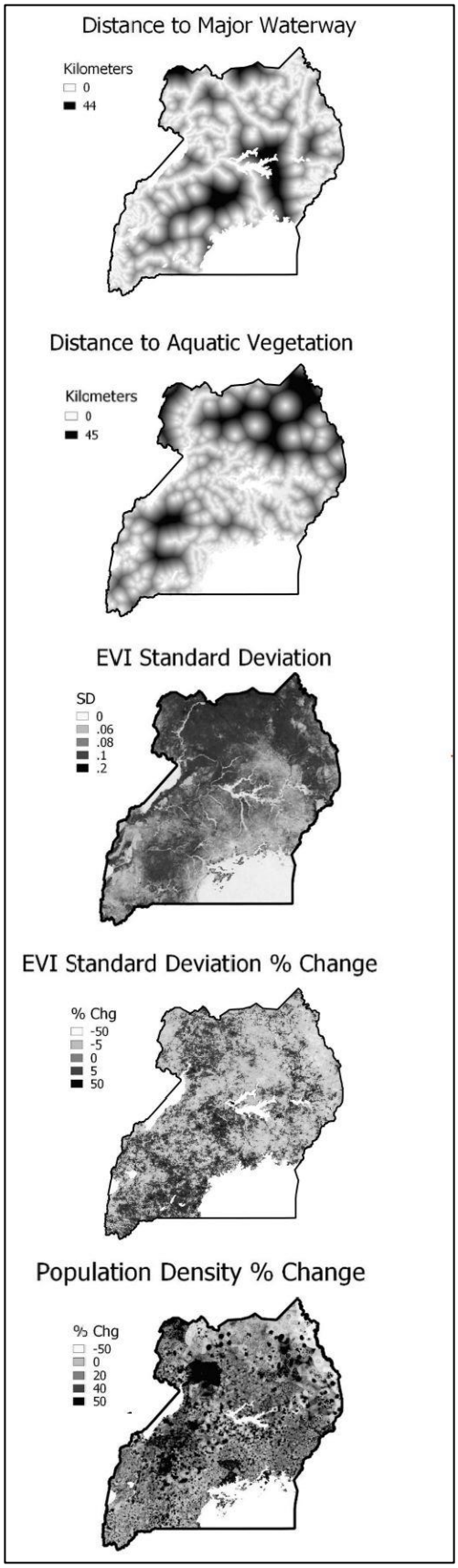

Figure 2. Distribution maps of predictors of Rift Valley Fever livestock seroprevalence. Geographic distributions of distance to a major waterway, distance to aquatic vegetation, SD of 8 year monthly average EVI, percent change in EVI SD over 8 years, and percent change in population density.

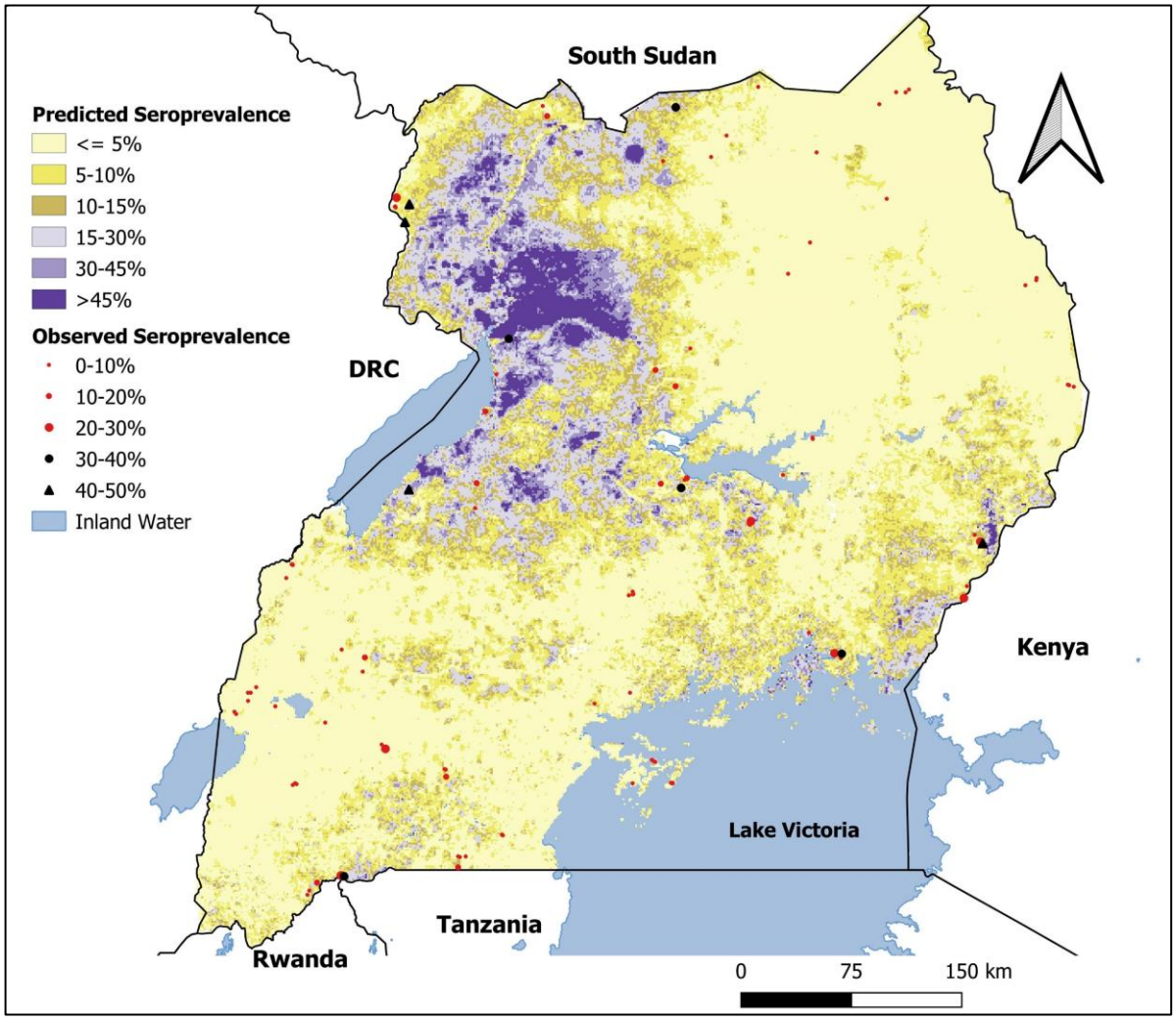

Figure 3. Predicted seroprevalence of Rift Valley Fever among livestock across Uganda. Predictions were based on geostatistical model fit to livestock sampling data, distance to a major waterway, distance to aquatic vegetation, 8-year Enhanced Vegetation Index (EVI) monthly standard deviation, 8-year percent change in EVI, and 8-year percent change in population density.

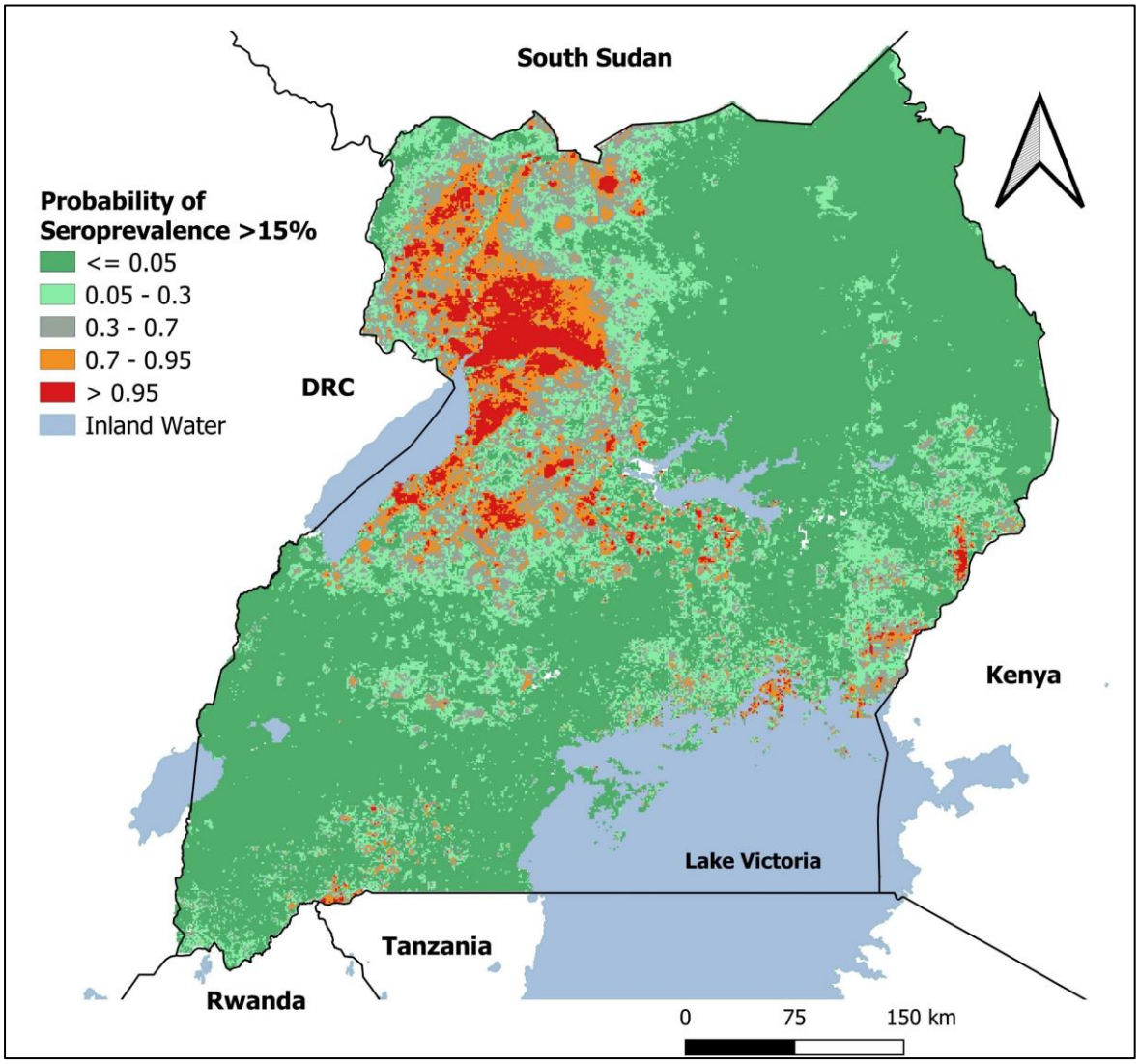

Figure 4. Rift Valley Fever Probability Map. Probability that seroprevalence of Rift Valley Fever among Uganda livestock exceeds 15%.

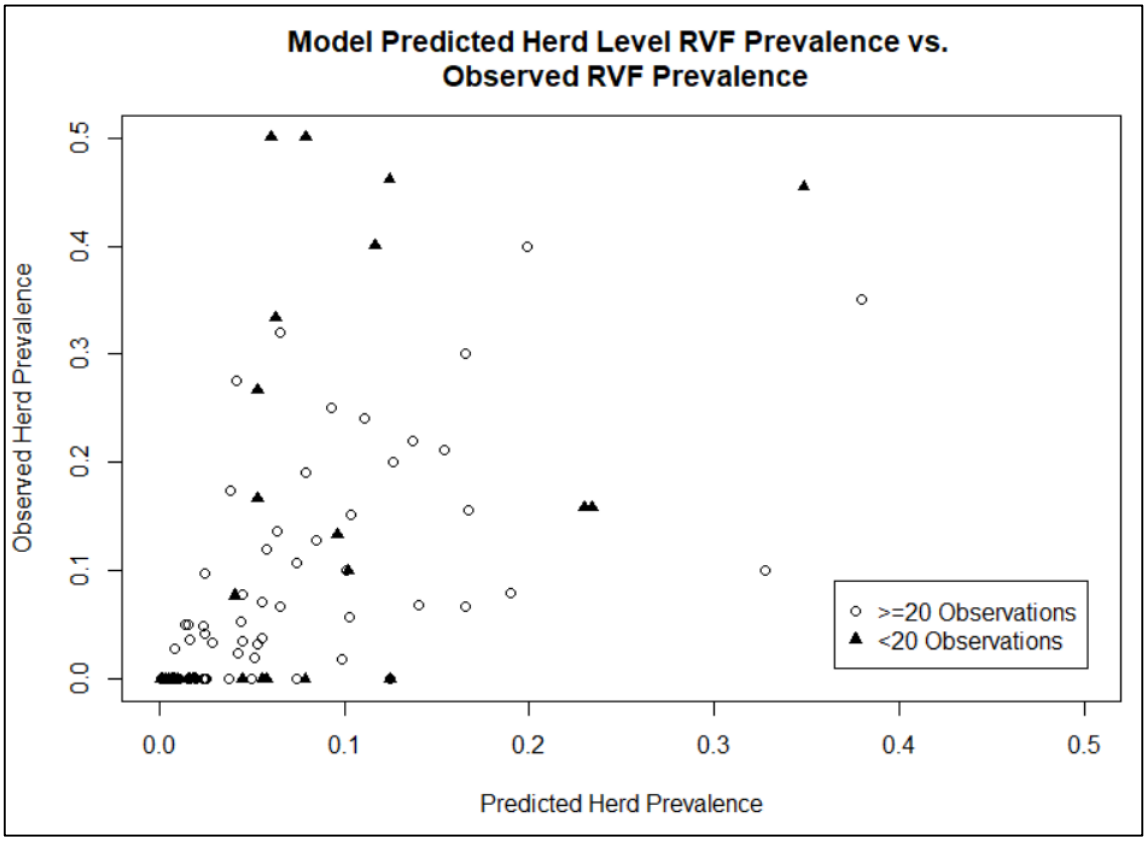

Figure 5. Predicted Rift Valley Fever seroprevalence compared to observed. Predicted RVF seroprevalence at points of observation compared to the observed seroprevalence from sampling. Triangular points represent herds with low sample size and unstable data, while circular points represent herds with a larger sample size.

Variable	Coefficient (Median)	Standard Error	0.025 CI	0.975 CI	P-value
Intercept	-5.22	1.37	-7.91	-2.53	0.0001
Distance to Major Waterway	-0.03	0.02	-0.07	0.01	0.12
Distance to Aquatic Vegetation	-0.03	0.02	-0.07	0.01	0.08
EVI SD	25.69	12.23	1.72	49.66	0.04*
EVI SD % Change	0.04	0.02	0.00	0.08	0.004**
Population Density % Change	0.02	0.01	0.00	0.04	0.006**
log(sigma^2)†	0.74	0.64	-0.51	1.99	-
log(phi)††	-0.18	0.54	-1.24	0.88	-
log(tau^2) †††	0.12	1.31	-2.45	2.69	-

Table 1. Model parameter estimates. Parameter estimates for the association between Rift Valley Fever seroprevalence and distance to the nearest waterway, distance to aquatic vegetation, enhanced vegetation index (EVI) annual standard deviation (SD), EVI SD percent change, population density percent change, and covariance parameters from a generalized linear geostatistical model using model-based geostatistics.

Abbreviations: EVI SD = Enhanced Vegetation Index

†Variance of the Gaussian process

††Scale of the spatial correlation

†††Variance of the nugget effect